Influence of synthesis route on morphology and conduction behavior of $BaCe_{0.8}Y_{0.2}O_{3-\delta}$

Pooja Sawant · S. Varma · B. N. Wani · S. R. Bharadwaj

Abstract In this article, the role of the preparation route and calcinations temperature on the thermal expansion and conductivity of $BaCe_{0.8}Y_{0.2}O_{3-\delta}$ (BCY) has been studied. In particular, the samples were synthesized by means of the solid-state reaction and by a sol–gel route. BCY has been suggested as proton conducting electrolyte for intermediate-temperature solid oxide fuel cells (IT-SOFCs). Proton conductivity strongly depends on the densification of the material as well as the crystal structure, which is generally influenced by the preparation procedure. It was found that a single phase material could be achieved at 1000 °C for the samples prepared through the sol–gel route with ∼96% packing density. In case of ceramic route, single phase could be obtained at higher temperatures (1200 °C) and does not lead to good density values. The ceramic synthesis produces BCY material in cubic symmetry where as the gel–citrate complexation route leads to homogenous orthorhombic BCY. The conductivity measurements of sample synthesized by two different routes were investigated by means of impedance spectroscopy and electron microscopy. A comparative study of thermal expansion behavior of BCY synthesized by different route was carried out.

Keywords Solid oxide fuel cells · Electrolyte · Barium cerate · Thermal expansion · Conductivity

P. Sawant · S. Varma · B. N. Wani (✉) · S. R. Bharadwaj
Chemistry Division, Bhabha Atomic Research Centre,
Mumbai 400085, India
e-mail: bnwani@barc.gov.in

Introduction

Intermediate-temperature solid oxide fuel cells (IT-SOFCs) have attracted considerable attention worldwide for their high efficiency and low environmental impact and played an important role in the hydrogen fuel economy [1–4]. Since Iwahara et al. [5–7] have found that some perovskite oxides show excellent protonic conductivity at intermediate temperatures hence they have become promising electrolyte candidates for the IT-SOFCs [8, 9]. During the past two decades, the rare earth-doped $BaCeO_3$ and $BaZrO_3$ have received substantial attentions, in which the trivalent rare earth elements are used as dopants to introduce oxygen vacancies [10–12]. Y-doped $BaCeO_3$ (BCY) has been intensively investigated due to their excellent proton conductivity at intermediate temperature [13–16]. However, one of the main limitations of such materials is to prepare dense ceramics. Many efforts have thus been made to prepare dense materials, but these hardly led to totally convincing results. The reported BCY powders were prepared mostly using conventional solid-state reactions since the processes are simple and cost-effective. In fact, powders prepared by solid-state reaction requires very high sintering temperatures (∼1200 °C) with treatments like intermittent grindings to obtain relative densities higher than 90%. However, using these reactions it is difficult to obtain super-fine ceramic powders with homogeneous composition, uniform shape, and size because of poor raw materials dispersion by physical mixing and relatively high sintering temperature for phase formation. Soft chemical methods led to powders with density values ∼95% with excellent properties can be easier to obtain by sintering uniform nanopowders when compared with the use of irregular micrometer sized powders [17]. It is well known that soft chemical routes such as gel combustion [18, 19],

modified Pechini method [20–22], and oxalate co-precipitation methods [23, 24] exhibit advantage of good homogeneity, narrow size and shape distribution, less time consumption, and lower sintering temperature for pure phase formation over the solid-state methods.

In this investigation, effect of synthesis route on various chemical–physical properties of the material such as grain size, density, porosity, structure, proton conductivity (σ), and thermal expansion behavior have been studied.
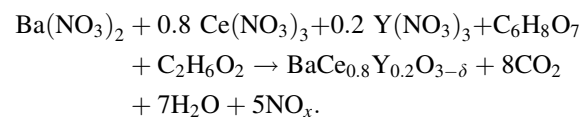
Experimental

Synthesis

$BaCe_{0.8}Y_{0.2}O_{3-\delta}$ (BCY) sample was prepared by a conventional solid-state reaction and sol–gel route. All the chemicals used were of high purity ($\sim99.6\%$) of Aldrich Chemicals. In case of solid-state route, stoichiometric amounts of $BaCO_3$, CeO_2, and Y_2O_3 were mixed together using mortar–pestle and heated at 900 °C for 2 days. The reaction products were reground, pressed into pellets by isostatic pressure, and heated at 1200 °C for 24 h. The final sintering of the pellets was done at 1400 °C for 10 h.

$$BaCO_3 + 0.8\ CeO_2 + 0.1\ Y_2O_3$$
$$\rightarrow BaCe_{0.8}Y_{0.2}O_{3-\delta} + CO_2 \uparrow.$$
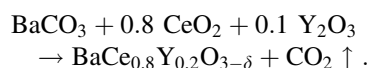
The BCY compound was also prepared by sol–gel method using citric acid monohydrate (CA) as chelating agent and ethylene glycol (EG) as a solvent. $Ce(NO_3)_3 \cdot 6H_2O$, $Ba(NO_3)_2$, and $Y(NO_3)_3 \cdot 3H_2O$ were used as starting materials. The molar ratio of CA to the total metal cations content was taken as 2:1. First, all the metal nitrates were dissolved in minimum volume of EG, and then CA was added to reaction mixture and stirred well to obtain transparent chelating solution. There was no precipitation during mixing of citric acid with metal nitrate solution as the pH of the solution was not varied. The solution was heated to 180 °C under continuous stirring to remove excess of water and convert it to a transparent viscous gel. On further heating, the gel was converted in a pale yellow ash. The resulting ash-like material was calcined at 800 °C for about 12 h. This powder was further pelletized and heated at 1000 °C for 12 h. The final sintering was done at 1400 °C for 10 h assuming complete combustion, the overall reaction between barium, cerium, and yttrium nitrate to form BCY can be written as:

$$Ba(NO_3)_2 + 0.8\ Ce(NO_3)_3 + 0.2\ Y(NO_3)_3 + C_6H_8O_7$$
$$+ C_2H_6O_2 \rightarrow BaCe_{0.8}Y_{0.2}O_{3-\delta} + 8CO_2$$
$$+ 7H_2O + 5NO_x.$$

Phase identification of samples synthesized by solid-state and sol–gel route was done by employing room temperature (RT) powder X-ray diffraction (XRD) technique on Philips diffractometer (PW 1729) with Ni-filtered Cu-Kα radiation and using silicon as external standard. The resulting powders were axially pressed in form of pellets of 10 mm diameter and sintered at 1000 °C for 10 h in air in case of powders synthesized by the sol–gel method and at 1200 °C for 24 h for samples obtained by the solid-state reaction. Sample density was estimated by Archimedes' method and compared with the theoretical density based on crystal lattice parameters. Morphologies of fracture surface of sintered pellets were determined using AIS 210 scanning electron microscope (Mirero Inc., Korea) coupled to an energy dispersive X-ray (EDAX) detector.

Thermal expansion

The thermal expansion of BCY was measured from 100 to 500 °C in dry argon atmosphere, using a quartz dilatometer (TMA 92 from Setaram) with digital micrometer. The micrometer sensitivity was 1 μm. The measurements were conducted during heating with a heating rate of 10 °C min^{-1}. The thermal expansion coefficient (TEC), α, was determined by graphic differentiation of the temperature dependence of the samples' expansion:

$$\alpha = \frac{1}{L_0}\frac{dL}{dT},$$

where L_0 is the sample's length at room temperature.

AC impedance measurement

The BCY electrolyte pellets were prepared by pressing the BCY powders at 1.5 tonnes in a 10 mm diameter die and subsequently sintered at 1400 °C for 10 h. Platinum paste was applied on each side of the sintered pellet to form electrodes, and then they were heated at 600 °C for 4 h to remove organic binders. The conductivity of BCY electrolyte was measured in humidified nitrogen gas flow using AC impedance spectrometer (Solartron 1260) in the frequency range from 0.1 Hz to 10 MHz and the applied ac voltage of 100 mV. Before each electrical measurement, the sample was equilibrated at constant temperature for 30 min. Both, Zplot 2.9b and ZView 2.9b softwares associated with the Solartron analyser were used to collect and analyze the impedance spectra of the BCY samples.

Results and discussion

X-ray diffraction

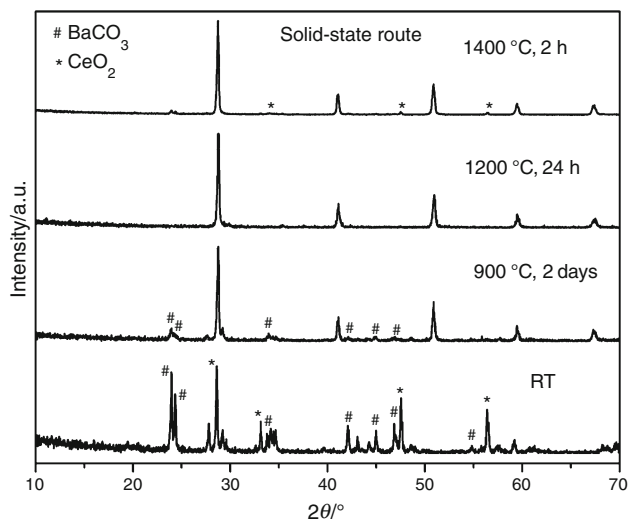Figure 1 shows the XRD patterns of BCY sample prepared by ceramic route and calcined at different temperatures.

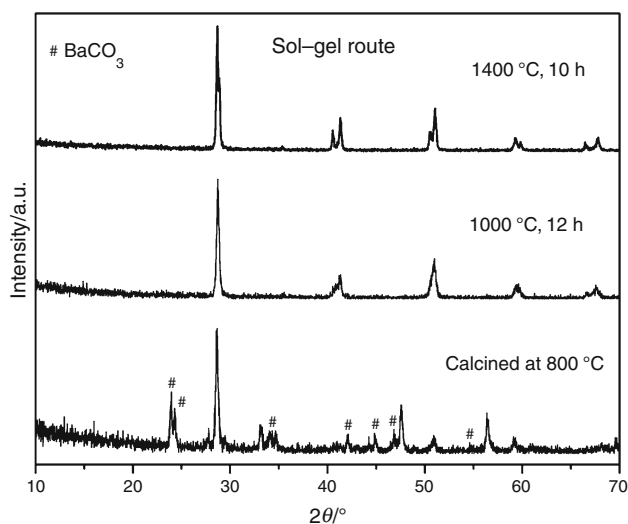**Fig. 1** XRD patterns of BCY synthesized by ceramic route at different temperatures

Fig. 2 XRD patterns of BCY synthesized by sol–gel route at different temperatures

Fig. 3 SEM micrographs of BCY synthesized by different routes: **a** solid-sate and **b** sol–gel

XRD pattern of room temperature mixture indicates the presence of $BaCO_3$, CeO_2, and Y_2O_3 in the sample. When the sample was heated to 900 °C, XRD pattern shows peaks due to Ba–Ce–Y oxide along with $BaCO_3$ indicating that the reaction is incomplete. On further heating to 1200 °C for 24 h single phase BCY perovskite has been obtained. This material when further heated to 1400 °C and cooled back to room temperature shows additional lines due to CeO_2 as minor impurity phase. This suggests that sample heated at 1400 °C is rich in Ba content as compared to ceria content.

In case of sol–gel route, XRD patterns of the precursor of BCY sample heated at different temperatures are given in Fig. 2. It indicates that single phase BCY can be obtained from sol–gel synthesis by heating at 1000 °C for 12 h and it is stable even if it is further heated to 1400 °C. To confirm this
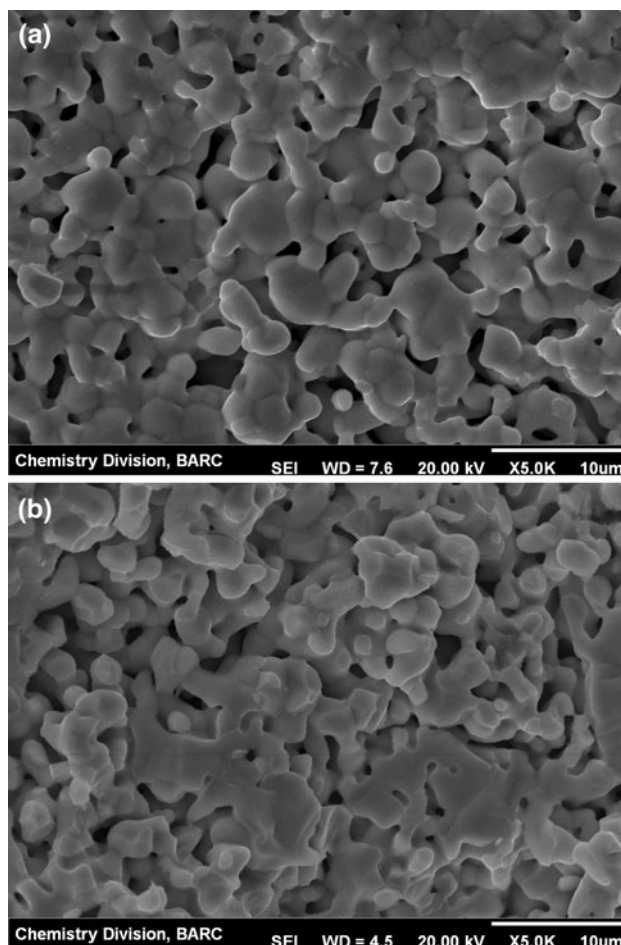
Ba analysis was done using EDAX analyzer. As compare to solid-state route synthesized material, sol–gel synthesized material shows barium deficiency. Lattice parameters of BCY prepared by both the routes were generated on the basis of $BaCeO_3$ structure. For ceramic route synthesized material it was found to be cubic symmetry with $a = 4.3968 \pm 0.001$ Å and cell volume of 85 ± 1 Å^3. BCY when prepared by sol–gel route it was found to have orthorhombic symmetry with $a_0 = 8.911 \pm 0.04$ Å, $b_0 = 6.164 \pm 0.02$ Å, $c_0 = 6.218 \pm 0.02$ Å, and cell volume was 338.2 ± 2 Å^3. This cell parameters are comparable to that reported for $BaCe_{0.9}Y_{0.1}O_{2.95}$ (JCPDF 81-1386) where $a = 8.77$ Å, $b = 6.238$ Å, $c = 6.223$ Å, and cell volume $V = 340.55$ Å^3.

The XRD results of BCY clearly indicate that the two different crystallographic phases of BCY could be obtained by applying different synthesis route. Second, BCY can be prepared by sol–gel method at lower temperature relative to the conventional solid-state reaction synthesis. This is possible since in sol–gel case the metal ions were dissolved into the solution and chelated with citric acid that led to homogeneous distribution of the elements and thereby

Fig. 4 EDAX spectrum of
BCY sample prepared by
different routes: **a** solid-sate and
b sol–gel
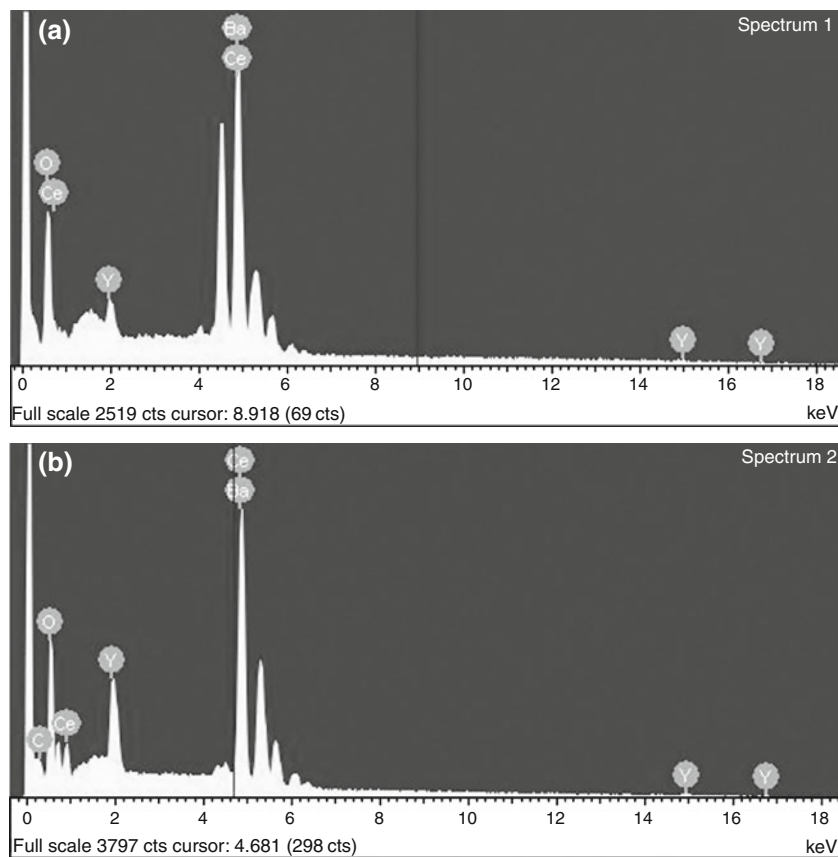
allowing ready formation of perovskite phase at relatively lower temperature.

The crystallite size of BCY powder obtained by sol–gel route at 1000 °C was calculated using Scherrer's formula and was found to be ~ 30 nm whereas those obtained from solid-state route at 1200 °C was found to be ~ 68 nm. The SEM images of fracture surface of well-sintered BCY pellet synthesized by solid-state route and sol–gel route are given in Fig. 3. SEM observations confirmed that the modified sol–gel process favoured the formation of denser sample with smaller particle size and have relatively few voids than the conventional solid-state route. Density of sample prepared by solid-state route was found to be 5.69 g cm^{-1} as compared to calculated density of cubic BCY 6.12 g cm^{-1}, indicating packing density value as 93%. Similarly for sol–gel synthesized BCY, density was found to be 5.86 g cm^{-1} and calculated one was 6.09 g cm^{-1} indicating packing density of 96.3%.

To confirm this EDAX analysis of BCY particle was carried out. The EDAX mapping BCY sample heated at 1400 °C showed an uniform elementary distribution of Ba, Ce, and Y (Fig. 4). In Table 1, atomic percentage of Ba and Ce concentrations were compared with calculated values for this BCY sample. It clearly indicates that BCY prepared by solid-state route was rich in Ba content as compared to sol–gel synthesized BCY.

Table 1 Atom percent distribution from EDAX analysis of BCY

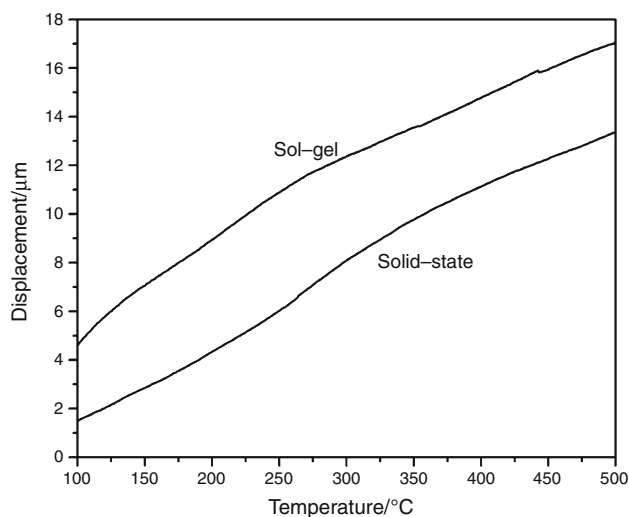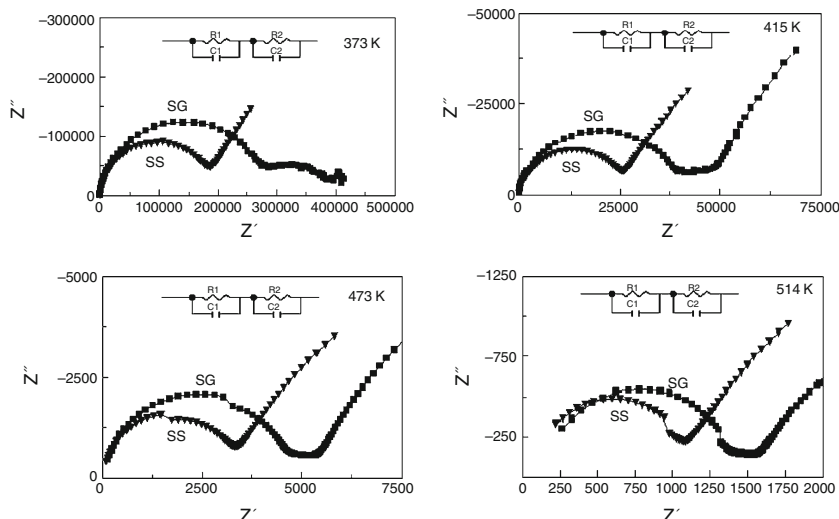| Sr no.	Element	As synthesized/atom%	EDAX/atom%	
			Solid state	Sol–gel
1	Ba	20.4	21.2	20.27
2	Ce	16.3	16.4	17.73

Fig. 5 Variation of linear thermal expansion versus temperature of BCY sample prepared by different routes

Fig. 6 IS plots at different temperatures for BCY sample prepared by sol–gel route (*SG*) and prepared by ceramic route (*SS*) sintered at 1400 °C
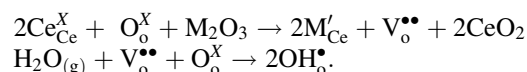

Thermal expansion

Thermal compatibility in the operation temperature regime is a critical issue for all the cell components of SOFCs. Linear thermal expansion data were collected on the dense pellets of BCY prepared by ceramic as well as sol–gel route at a heating rate of 10 K/min in the dry argon atmosphere in the temperature interval of 30–500 °C. BCY samples prepared by either ceramic or sol–gel route showed non-linear thermal expansion behavior (Fig. 5). The average linear TEC values for BCY samples prepared by ceramic route was found to be 14.13×10^{-6} K^{-1} which was lower than that prepared by sol–gel route (15.52×10^{-6} K^{-1}). The difference in TEC values obtained for samples prepared by two routes might be due to difference in structural symmetry namely cubic and orthorhombic. Even though, TEC values of BCY are lower than those of commonly used cathode materials for proton conducting fuel cell that is $Ba_{0.5}Sr_{0.5}Co_{0.2}Fe_{0.8}O_{3-\delta}$ (18.53×10^{-6} K^{-1}) [25] and it is closer to another set of cathode materials namely $La_{0.6}Sr_{0.4}Co_{0.2}Fe_{0.8}O_{3-\delta}$ (15.3×10^{-6} K^{-1}) [26].

Conductivity measurements

The AC impedance spectroscopy was employed to measure proton conductivity at lower temperatures (100–250 °C) to probe the relative contribution of bulk and grain boundary to the total conductivity of the samples prepared by different routes. Typical spectra in moist nitrogen atmosphere for BCY, prepared by ceramic route as well as by sol–gel route, are shown in Fig. 6. Overall feature of the spectrum is identical and can be modeled with the equivalent circuit shown as inset in Fig. 6. Two semi-circles are evident followed by a linear impedance variation at lower frequencies.

The higher frequency arc (lower Z' values) corresponds to phenomena occurring in the bulk of the electrolyte. The lower frequency (higher Z' values) linear impedance variation represents the behavior occurring at the electrode–electrolyte interface. An arc in the mid-frequency range can be assigned to grain boundary impedances. It is seen that two overlapping semicircles are obtained for solid-state synthesized BCY sample whereas semicircles for grain and grain boundary are evident in sol–gel synthesized BCY sample at lower temperature of ~ 473 K. As the temperature increases, these two semicircles could not be resolved and obtained as single semicircle similar to that of solid-state synthesized. The total electrical resistance determined from the impedance spectra is the sum of $R_{total} = R_{grain} + R_{grain\ boundary}$. The values of grain boundary resistance (R_{gb}) are less than the grain resistance (R_{g}). This indicates the presence of lower grain size and the absence of any detrimental impurity like silica which can lead to increase in R_{gb} contribution.

The mechanism of proton conduction in barium cerate-based materials, in which substitutions of Ce^{4+} by Y^{3+} cause the formation of oxygen vacancies and this determines its proton conductivity. Kroger–Vink notation of incorporation of trivalent dopants and subsequent incorporation of water/protons described as [27]:

$$2Ce_{Ce}^{X} + O_{o}^{X} + M_2O_3 \rightarrow 2M_{Ce}' + V_{o}^{\bullet\bullet} + 2CeO_2$$
$$H_2O_{(g)} + V_{o}^{\bullet\bullet} + O_{o}^{X} \rightarrow 2OH_{o}^{\bullet}.$$

Water from the gas-phase dissociates into a hydroxide ion and a proton, where oxygen vacancies are replaced by hydroxide ions and small protons forms a covalent bond with lattice oxygen. The following mechanism was proposed by Iwahara et al. [7] for proton conduction in perovskite oxides,
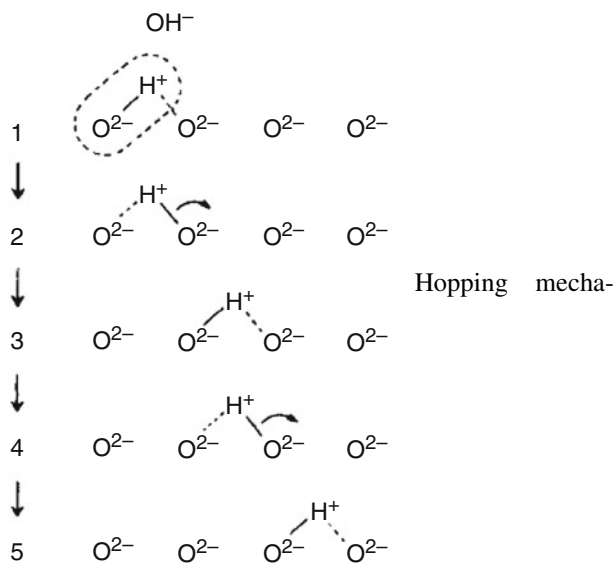
Hopping mecha-

nism of migration of proton from one oxygen ion to another nearest oxygen ion.

The bulk, grain boundary, and the total conductivities were calculated from the respective resistance value of the semicircles employing equivalent circuit as shown in Fig. 6 and the values are tabulated in Table 2. Figure 7 shows the variation of total conductivity as a function of temperature for BCY samples prepared by different routes. In both the cases, conductivity increases as the temperature increase (Table 2). BCY synthesized by ceramic route shows higher conductivity than sol–gel synthesized sample at lower temperature, but at higher temperature both samples shows comparable conductivities. The EDAX data for BCY samples prepared by solid-state and sol–gel route, as shown in Table 3, clearly exhibit that the samples prepared by the solid-state route are relatively richer in barium concentration compared to those prepared by sol–gel. This observation is found to be in agreement with reported data on influence of barium stoichiometry on proton conductivity. Ma et al. [28] have clearly delineated the decrease in
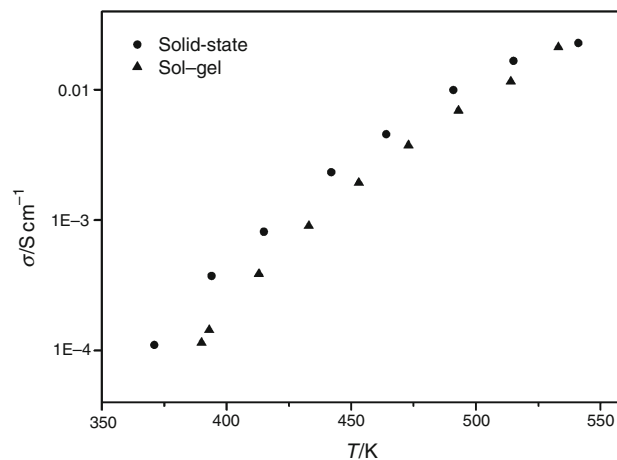

Fig. 7 Variation of total conductivity as a function of temperature for BCY samples prepared by different routes

Table 3 Activation energy for proton conduction of BCY

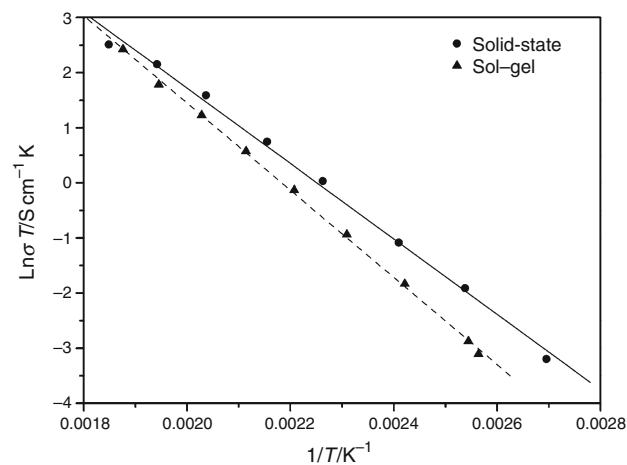|	Total E_a/eV	Grain E_a/eV	Grain boundary E_a/eV
Solid state	0.59	0.62	0.38
Sol–gel	0.68	0.65	0.62

Fig. 8 Arrhenius plot of BCY sample prepared by two different routes

conductivity as stoichiometry goes from Ba-rich to Ba-lean composition.

A comparative plot of log (σT) as a function of $1/T$ for two preparative methods is shown in Fig. 8. The samples exhibit apparent Arrhenius-type T dependencies of conductivities. The activation energies of the proton conductivity for grain, grain boundary, and total were calculated and listed in Table 3. For ceramic route synthesized BCY sample activation energies for bulk conduction was higher than that required for grain boundary conduction

Table 2 Proton conductivity values at different temperatures

Temp/K	Grain	Grain boundary	Total
Solid-state conductivity/S cm^{-1} × 10^{-3}			
373	0.12	2.45	0.11
415	0.85	18.25	0.82
464	5.17	38.15	4.55
514	21.28	78.23	16.73
Sol–gel conductivity/S cm^{-1} × 10^{-3}			
393	0.24	0.36	0.14
413	0.56	1.25	0.39
473	4.74	18.04	3.75
514	16.60	38.57	11.60

mechanisms. In case of sol–gel synthesized sample activation energies were almost same for grain and grain boundary conduction. This difference can be due to variations in microstructure as seen from the SEM micrographs.

Conclusions

Perovskites of the type $BaCe_{0.8}Y_{0.2}O_{3-\delta}$ can be prepared via ceramic as well as sol–gel route. When BCY is synthesized by sol–gel route, the calcinations temperature needed to obtain a single phase is ~1000 °C, 200 °C lower than required for preparation from a ceramic route (~1200 °C). This is potentially advantageous in terms of the cost of ceramic preparation. The bulk conductivities and activation energies determined by impedance spectroscopy method are, as expected, nearly identical for both preparative routes. There are, however, differences in the form of the impedance spectra for samples deriving from the two methods. These differences are attributed to variations in the microstructure of the ceramic as well as sol–gel prepared samples. The linear thermal expansion of BCY has been measured using TMA, showing nonlinear expansion behavior in the temperature range 100–500 °C.

The proton conductivity of $BaCe_{0.8}Y_{0.2}O_{3-\delta}$ sample prepared in this study is comparatively higher than those previously reported values, which makes the material a promising candidate as an electrolyte for intermediate temperature SOFCs.

References

1. Huijsmans JPP, Berkel FPF, Christie GM. Intermediate temperature SOFC—a promise for the 21st century. J Power Sources. 1998;71:107–10.
2. Zhu B, Albinsson I, Mellander BE, Meng G. Intermediate-temperature proton-conducting fuel cells—present experience and future opportunities. Solid State Ion. 1999;125:439–46.
3. Zhu B. Advantages of intermediate temperature solid oxide fuel cells for tractionary applications. J Power Sources. 2001;93:82–6.
4. Matsumoto H, Nomura I, Okada S, Ishihara T. Intermediate-temperature solid oxide fuel cells using perovskite-type oxide based on barium cerate. Solid State Ion. 2008;179:1486–9.
5. Iwahara H, Uchida H, Tanaka S. High temperature type proton conductor based on $SrCeO_3$ and its application to solid electrolyte fuel cells. Solid State Ion. 1983;9–10:1021–5.
6. Iwahara H, Uchida H, Ono K, Ogaki K. Proton conductors in sintered oxides based on $BaCeO_3$. J Electrochem Soc. 1988;135:529–33.
7. Iwahara H. Proton conducting ceramics and their applications. Solid State Ion. 1996;86–88:9–15.
8. Kreuer KD. Proton conducting oxides. Annu Rev Mater Res. 2003;33:333–59.
9. Schober T. Applications of oxidic high-temperature proton conductors. Solid State Ion. 2003;162–163:277–81.
10. Norby T, Larring Y. Concentration and transport of protons in oxides. Curr Opin Solid State Mater Sci. 1997;2:593–9.
11. Bonanos N. Oxide-based protonic conductors: point defects and transport properties. Solid State Ion. 2001;145:265–74.
12. Iwahara H. Technological challenges in the application of proton conducting ceramics. Solid State Ion. 1995;77:289–98.
13. Coors WG, Readey DW. Proton conductivity measurements in yttrium barium cerate by impedance spectroscopy. J Am Ceram Soc. 2002;85(11):2637–40.
14. Maekawa H, Ukei Y, Morota K, Kashii N, Kawamura J, Yamamura T. High temperature proton NMR study of yttrium doped barium cerates. Solid State Commun. 2004;130:73–7.
15. Giannici F, Longo A, Deganello F, Balerna A, Arico AS, Martorana A. Local environment of barium, cerium and yttrium in $BaCe_{1-x}Y_xO_{3-\delta}$ ceramic protonic conductors. Solid State Ion. 2007;178:587–91.
16. Sneha BR, Thangadurai V. Synthesis of nano-sized crystalline oxide ion conducting fluorite-type Y_2O_3-doped CeO_2 using perovskite-like $BaCe_{0.9}Y_{0.1}O_{2.95}$ (BCY) and study of CO_2 capture properties of BCY. J Solid State Chem. 2007;180:2661–9.
17. Khani Z, Jacquin MT, Taillades G, Marrony M, Jones DJ, Roziere J. New synthesis of nanopowders of proton conducting materials. A route to densified proton ceramics. J Solid State Chem. 2009;182:790–8.
18. Jacquin M, Jing Y, Essoumhi A, Taillades G, Jones DJ, Rozière J. Flash combustion synthesis and characterisation of nanosized proton conducting yttria-doped barium cerate. J New Mater Electrochem Syst. 2007;10:243–8.
19. Taillades G, Jacquin M, Khani Z, Jones D, Marrony M, Roziere J. Development of proton conducting thin films from nanoparticulate precursors. ECS Trans. 2007;7:2291–8.
20. Scholten MJ, Schoonman J, Miltenburg JCV, Oonk HAJ. Synthesis of strontium and barium cerate and their reaction with carbon dioxide. Solid State Ion. 1993;61:83–91.
21. Pechini MP. Method of preparing lead and alkaline earth titanates and niobates and coating method using the same to form a capacitor. US Patent 3330697, 1967.
22. Lee DW, Won JH, Shim KB. Low temperature synthesis of $BaCeO_3$ nano powders by the citrate process. Mater Lett. 2003;57:3346–51.
23. Flint SD, Slade RCT. Comparison of calcium-doped barium cerate solid electrolytes prepared by different routes. Solid State Ion. 1995;77:215–21.
24. Chen F, Wang P, Sørensen OT, Meng G, Peng D. Preparation of Nd-doped $BaCeO_3$ proton-conducting ceramics by homogeneous oxalate coprecipitation. J Mater Chem. 1997;7:1533–9.
25. Wang Y, Wang S, Wang Z, Wen T, Wen Z. Performance of $Ba_{0.5}Sr_{0.5}Co_{0.8}Fe_{0.2}O_{3-\delta}$–CGO–Ag cathode for IT-SOFCs. J Alloys Compd. 2007;428:286–9.
26. Yang L, Liu Z, Wang S, Choi YM, Zuo C, Liu M. A mixed proton, oxygen ion, and electron conducting cathode for SOFCs based on oxide proton conductors. J Power Sources. 2010;195:471–4.
27. Kroger FA, Vink HJ. Relations between the concentrations of imperfections in crystalline solids. Solid State Phys. 1956;3:307–435.
28. Ma G, Matsumoto H, Iwahara H. Ionic conduction and nonstoichiometry in non-doped $Ba_xCeO_{3-\alpha}$. Solid State Ion. 1999;122:237–47.